MAGNETIC RESONANCE IN CHEMISTRY
Magn. Reson. Chem. 2004; **42**: 453–458
Published online 27 February 2004 in Wiley InterScience (www.interscience.wiley.com). DOI: 10.1002/mrc.1364

Solid-phase synthesis and ^{1}H and ^{13}C high-resolution magic angle spinning NMR of ^{13}C-labeled resin-bound saccharides

Nikolaus M. Loening,* Takuya Kanemitsu,† Peter H. Seeberger‡ and Robert G. Griffin

Department of Chemistry, Massachusetts Institute of Technology, Cambridge, Massachusetts 02139, USA

Received 27 August 2003; Revised 3 December 2003; Accepted 17 December 2003

We show how high-resolution magic angle-spinning NMR spectroscopy can be used to characterize ^{13}C-labeled saccharides that have been prepared using solid-phase synthesis techniques while they are still bound to a solid-support resin. With the use of ^{13}C-labeled glucose as the starting material, we have successfully synthesized mono-, di- and trisaccharides with uniform ^{13}C labeling of the saccharide rings. Using these materials, we have been able to assign the ^{13}C and ^{1}H spectra and to characterize various impurities on the resin beads. Copyright © 2004 John Wiley & Sons, Ltd.

KEYWORDS: NMR; ^{1}H NMR; ^{13}C NMR; oligosaccharides; high-resolution magic angle spinning; solid support; gel phase; carbohydrates

INTRODUCTION

Solid-phase synthesis techniques have proven to be useful methods for generating oligopeptides,[1,2] oligonucleotides[3] and, more recently, oligosaccharides.[4,5] However, characterization of reaction products by NMR spectroscopy while they are still resin bound is difficult because the presence of the solid support reduces the spectral resolution. Although the use of high-resolution magic angle spinning (HR-MAS) techniques[6–8] can drastically improve the resolution, the resonances in HR-MAS spectra are still broad relative to conventional solution-state NMR spectra. Therefore, spectral overlap often complicates the characterization of resin-bound products; this is particularly relevant in the analysis of oligosaccharides, where the ^{1}H resonances are dispersed over a relatively limited range of chemical shifts. Although high-resolution solution-state NMR spectra of reaction products can be acquired after cleaving them from the solid support, the analysis of products while they are still resin bound is more useful as this allows reaction products and intermediates to be identified during the course of a synthesis rather than only at the end.

In this paper, we describe the synthesis of ^{13}C-labeled mono- and oligosaccharides using solid-phase synthesis techniques along with the application of HR-MAS ^{1}H and ^{13}C NMR to these samples. Previous efforts towards the study of resin-bound saccharides using HR-MAS NMR were only partially successful in assigning the ^{1}H and ^{13}C spectra[9] or focused on monitoring ^{13}C-labeled[10,11] or ^{19}F-containing[12–14] protecting groups to track the progression of a synthesis. By including ^{13}C labels on the saccharide itself, we are able to use the additional chemical shift dispersion from the ^{13}C spectrum to disentangle and assign the poorly resolved ^{1}H spectrum.

*Correspondence to: Nikolaus M. Loening, Department of Chemistry, Lewis & Clark College, 0615 SW Palatine Hill Road, Portland, Oregon 97219, USA. E-mail: loening@lclark.edu
†Present address: Division of Organic and Bioorganic Chemistry, Kyoritsu College of Pharmacy, Shibakoen 1-5-30, Minatoku, Tokyo 105, Japan.
‡Present address: Laboratory for Organic Chemistry, ETH Hönggerberg, HCI F315, Wolfgang-Pauli-Strasse 10, CH-8093 Zürich, Switzerland.
Contract/grant sponsor: NIH NIBIB; Contract/grant number: EB002026.

EXPERIMENTAL

Compounds

The starting material for the solid-phase synthesis ([$^{13}C_6$]dibutyl-3,4-di-*O*-benzyl-6-*O*-levulinoyl-2-*O*-pivaloyl-D-glucopyranosyl phosphate, **7**) was synthesized starting from [$^{13}C_6$]-D-glucose as shown in Fig. 1. The resulting ^{13}C-labeled starting material was then used in the stepwise solid-phase reaction scheme shown in Fig. 2 to generate ^{13}C-labeled mono-, di- and trisaccharide samples. The solid support used for the synthesis was 1% divinylbenzene cross-linked chloromethyl polystyrene resin (Merrifield resin). Polystyrene resins have become the standard support for oligosaccharide solid-phase synthesis owing to their ready availability, synthetic versatility and compatibility with a wide range of solvents and reagents. Although other polymeric supports (such as the polyethylene glycol cross-linked polymeric supports POEPS and POEPOP) facilitate on-resin analysis, they are not widely used for the routine synthesis of oligosaccharides. All chemicals were of reagent grade and used as supplied except as noted. Dichloromethane and tetrahydrofuran were purified using a J.T. Baker Cycle-Tainer Solvent Delivery System. Solutions were evaporated under reduced pressure at a bath temperature not exceeding 40 °C. Column chromatography was performed using a forced flow of the indicated solvent on Sigma H-type silica (10–40μm).

3,4,6-O-Acetyl-D-arabino-hex-1-enitol (2)

A mixture of [$^{13}C_6$]-D-glucose (**1**, 1000 mg, 5.73 mmol) and acetic anhydride (5 ml, 52.9 mmol) in pyridine (10 ml) was stirred at room temperature for 3 h, after which the reaction mixture was

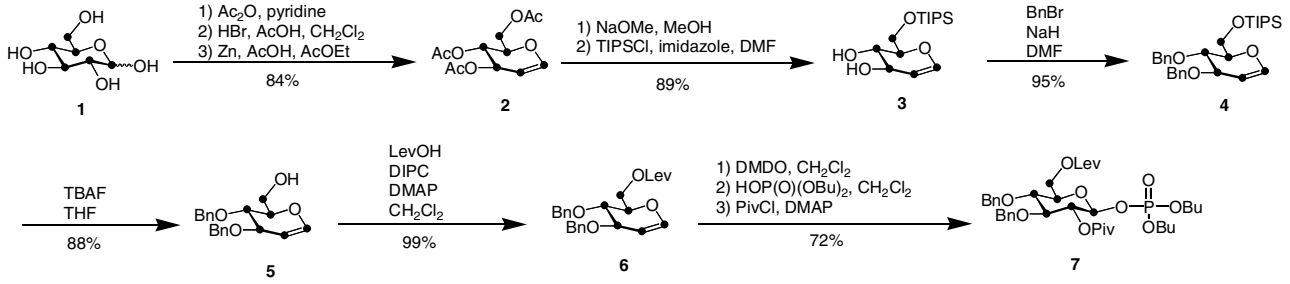

Figure 1. Synthesis of the ^{13}C-labeled glycosylating agent (**7**). The starting material (**1**) was uniformly ^{13}C labeled, as indicated by the dots in the structure. As a result, **7** was ^{13}C labeled around the glucose ring. See text for further details of the synthesis.

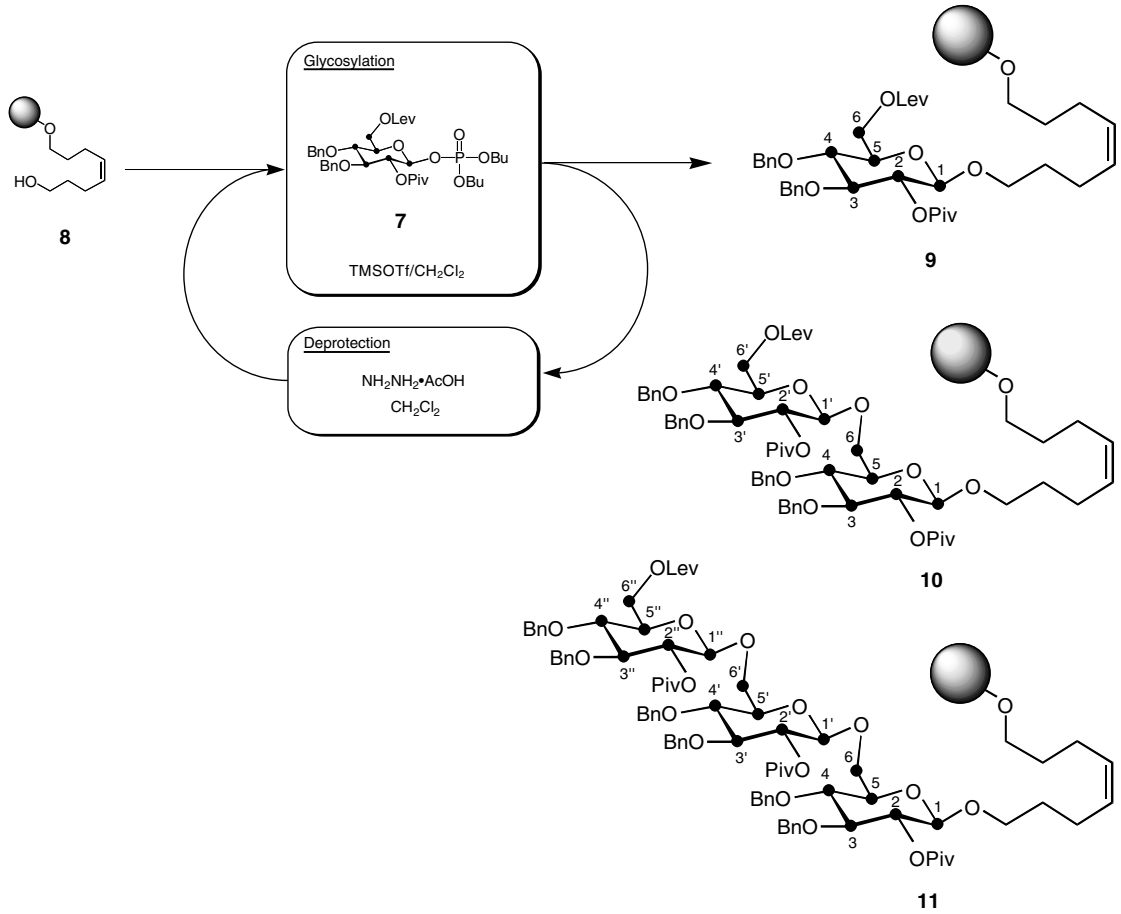

Figure 2. Solid-phase synthesis of the ^{13}C-labeled mono-, di- and trisaccharides (**9**, **10** and **11**). The labeled sites on the glucose rings are indicated by dots and by the numbering. Further details of these syntheses are provided in the text.

concentrated. The resulting peracetylglucose was dissolved in CH_2Cl_2 (20 ml) and cooled to 0 °C. A 33% HBr–AcOH mixture (4 ml) was added slowly and the solution was stirred at 0 °C for 3 h. After allowing the solution to warm to room temperature, it was stirred for an additional 3 h. The reaction mixture was poured into ice-cold aqueous $NaHCO_3$, eluted with CH_2Cl_2, washed with H_2O, dried over $MgSO_4$, filtered and finally concentrated to provide glycosyl bromide. The compound was dissolved with ethyl acetate (10 ml) and cooled to 0 °C. A suspension of Zn dust (3.8 g), $CuSO_4{\cdot}5H_2O$ (50 mg) and AcONa (250 mg) in 60% AcOH–H_2O (26 ml) was added to the reaction solution and stirred at 0 °C for 1 h and at room temperature for 1 h. After the reaction was complete, the suspension was filtered through a pad of Celite. The resulting filtrate was eluted with ethyl acetate, washed with aqueous $NaHCO_3$ and H_2O, dried over $MgSO_4$, filtered and concentrated. The residue was purified on a silica gel column using hexane–ethyl acetate (75 : 25) as eluent to provide **2** (1474 mg, 84%).

6-O-Triisopropylsilyl-D-arabino-hex-1-enitol (3)
Compound **2** (1220 mg, 4.39 mmol) was dissolved in MeOH (18 ml). Sodium methoxide (0.5 M in MeOH, 2 ml) was added to this solution and stirred at room temperature for 2 h, after which the reaction mixture was neutralized with Amberlite IR-120 (H^+), filtered and concentrated. This concentrate was dissolved with DMF (10 ml) and cooled to 0 °C. Triisopropylsilyl chloride (1.0 ml, 4.67 mmol) and imidazole (580 mg, 8.52 mmol) were added to this solution, after which the mixture was stirred at 0 °C for 2 h and concentrated. The residue was purified using silica gel column chromatography with toluene–acetone (80 : 20) as eluent to provide **3** (1204 mg, 89%).

3,4-Di-O-benzyl-6-O-triisopropylsilyl-D-arabino-hex-1-enitol (4)
Compound **3** (1200 mg, 3.89 mmol) was dissolved in DMF (20 ml) and cooled to 0 °C. NaH (60% oil dispersion, 470 mg, 11.75 mmol) was added and the resulting solution was stirred at 0 °C for 1 h. BnBr (1.86 ml, 15.55 mmol) was added and the mixture was stirred at 0 °C for 2 h. After the reaction was complete, the excess of

NaH was decomposed by MeOH. The mixture was diluted with CH_2Cl_2, washed with H_2O twice, dried over $MgSO_4$, filtered and concentrated. The residue was purified using silica gel column chromatography with hexane–ethyl acetate (15 : 1) as eluent to provide **4** (1805 mg, 95%).

3,4-Di-O-benzyl-D-arabino-hex-1-enitol (5)
Compound **4** (1780 mg, 3.64 mmol) was dissolved in THF (10 ml) and cooled to 0 °C. A 1.0 M solution of TBAF in THF (5.5 ml, 5.5 mmol) was added and the resulting solution was stirred for 1 h at 0 °C and for 3 h at room temperature. The reaction mixture was diluted with CH_2Cl_2, washed with H_2O twice, dried over $MgSO_4$, filtered and concentrated. The residue was purified using silica gel column chromatography with hexane–ethyl acetate (75 : 25) as eluent to provide **5** (1070 mg, 88%).

3,4-Di-O-benzyl-6-O-levulinoyl-D-arabino-hex-1-enitol (6)
A mixture of **5**, levulinic acid (0.64 ml, 6.23 mmol), DIPC (0.98 ml, 6.21 mmol) and DMAP (38 mg, 0.31 mmol) in CH_2Cl_2 was stirred at 0 °C for 2 h. The reaction mixture was purified using silica gel column chromatography with toluene–acetone (90 : 10) as eluent to give **6** (1316 mg, 99%).

Dibutyl 3,4-di-O-benzyl-6-O-levulinoyl-2-O-pivaloyl-D-glucopyranosyl phosphate (7)
Compound **6** (427 mg, 0.992 mmol) was dissolved in CH_2Cl_2 (10 ml) and cooled to 0 °C. A solution of dimethyldioxirane in acetone (0.08 M, 19 ml, 1.5 mmol) was added and the reaction mixture was stirred at 0 °C for 20 min. The solvent was then removed using a stream of nitrogen. After the remaining residue had been dried *in vacuo* at 0 °C for 10 min, 10 ml of CH_2Cl_2 were added to dissolve the residue. The resulting solution was cooled at −78 °C for 15 min. At this temperature, a solution of dibutyl phosphate (0.235 ml, 1.19 mmol) in CH_2Cl_2 (10 ml) was added dropwise over a period of 5 min. The reaction mixture was then warmed to 0 °C, at which point DMAP (485 mg, 3.97 mmol) and pivaloyl chloride (0.245 ml, 1.99 mmol) were added to the solution. The solution was then allowed to warm to room temperature over 1 h and hexane–ethyl acetate (1 : 1) was added. The reaction mixture was filtered through a short silica gel column and concentrated. The residue was purified using silica gel column chromatography with hexane–ethyl acetate (60 : 40) as eluent to afford **7** (529 mg, 72%).

Glycosylation reaction on solid phase. General procedure
A mixture of octenediol linker-bound resin **8** (300 mg, ~0.15 mmol, 1 equiv.) and the glycosylating agent **7** (222 mg, 0.3 mmol, 2 equiv.) in anhydrous CH_2Cl_2 (10 ml) was shaken at room temperature for 15 min. This suspension was then cooled to −78 °C, at which point a solution of 0.5 M trimethylsilyltrifluoromethanesulfonic acid in CH_2Cl_2 (0.6 ml, 0.3 mmol, 2 equiv.) was added. The suspension was shaken under a nitrogen atmosphere at a temperature between −78 and −50 °C for 1 h. The resin was then washed with CH_2Cl_2, MeOH, THF and CH_2Cl_2. This procedure was repeated twice.

Deprotection reaction on solid phase. General procedure
A mixture of carbohydrate-bound resin **9** (277 mg, ~0.13 mmol, 1 equiv.), acetic anhydride (0.05 ml, 0.53 mmol, 4 equiv.) and DMAP (5 mg, 0.04 mmol, 0.3 equiv.) in pyridine (10 ml) was shaken at room temperature for 2 h. The resin was then washed with pyridine–acetic acid (3 : 2). A solution of 0.25 M N_2H_4·HOAc in pyridine–acetic acid (3 : 2) (10 ml, 2.5 mmol) was added to the resin and the suspension was shaken at room temperature for 30 min. The resin was then washed with pyridine–acetic acid (3 : 2), 0.2 M AcOH in THF, THF and CH_2Cl_2. This procedure was repeated twice.

Spectroscopy

The ^1H and ^{13}C NMR spectra of the resin-bound mono-, di-, and trisaccharides (**9**, **10**, and **11** in Fig. 2) were acquired on a Bruker DRX600 spectrometer operating at 600 MHz for ^1H and 125 MHz for ^{13}C and equipped with a $^1H/^{13}C$ HR-MAS probe. The samples were swollen in $CDCl_3$ (which also served as the lock solvent and reference) prior to packing the swelled resin into 4 mm zirconium rotors. Swelling the resin is crucial for obtaining high-resolution spectra as it is only in the gel phase that the resin is sufficiently mobile on a molecular scale to average effects due to dipolar couplings and chemical shift anisotropy. Even with a swelled resin, residual dipolar couplings and magnetic susceptibility gradients due to the solid–liquid interfaces in the sample substantial broaden the spectrum. Fortunately, these effects can be greatly attenuated by spinning the sample about the magic angle. The resulting HR-MAS spectra are very similar to solution-state NMR spectra in terms of information content (isotropic chemical shifts and scalar couplings) and, in favorable cases, resolution. For our experiments, the samples were spun at a frequency of 6 kHz to ensure that any sidebands were outside the 0–10 ppm chemical shift range of the ^1H spectra.

The composite pulse decoupling sequence WALTZ-16[15,16] was used for both ^1H decoupling ($\omega_1/2\pi = 2.5$ kHz) and ^{13}C decoupling ($\omega_1/2\pi = 4.2$ kHz). HSQC spectra[17] were measured using 2048 (t_2) × 512 (t_1) points and zero-filled once in each dimension prior to Fourier transformation. With 16 scans per increment and a recycle delay of 1 s, the experiment time for each HSQC experiment was 2.3 h. INADEQUATE spectra[18] were measured using 2048 (t_2) × 256(t_1) points and zero-filled once in each dimension prior to Fourier transformation. With 64 scans per increment and a recycle delay of 1 s, the experiment time used to acquire each INADEQUATE spectrum was 4.6 h. The length of the spin-echo period at the beginning of the INADEQUATE sequence was set so that 50 Hz ^{13}C–^{13}C scalar couplings resulted in the most efficient generation of double quantum coherences. INADEQUATE experiments optimized for weaker ^{13}C–^{13}C couplings (33 Hz) produced similar results.

All spectra were recorded at room temperature (25 °C).

RESULTS AND DISCUSSION

The ^1H HR-MAS spectrum of **9** [Fig. 3(a)] highlights the relatively broad lines that sometimes occur with resin-bound samples. Resonances due to protons on the saccharide ring appear between 3 and 5.5 ppm; the strong background signals that appear between 1–2.5 and 6–8 ppm are primarily due to the resin. As the ring protons are coupled to ^{13}C nuclei (via both one-bond and longer range couplings), the use of ^{13}C decoupling improves both the spectral resolution and the sensitivity [Fig. 3(b)]. Even so, there are still a number of resonances that overlap the ring protons; these can be excluded from the spectrum by incorporating a ^{13}C filter based on two INEPT transfers.[19] By using such a ^{13}C filter in the pulse sequence, the ^1H spectrum [Fig. 3(c)] only includes protons that are directly bound to ^{13}C nuclei and, as a result, the seven ring protons in the monosaccharide sample (**9**) can almost be completely resolved. Unfortunately, the ^1H linewidths are ~50 Hz, even with ^{13}C decoupling, so the resonances in the much more congested ^1H spectra from the disaccharide [**10**, Fig. 3(d), 14 resonances are expected] and trisaccharide [**11**, Fig. 3(e), 21 resonances are expected] samples cannot be straightforwardly resolved.

The ring protons are difficult to resolve because the peaks are dispersed by their chemical shifts over a range of only

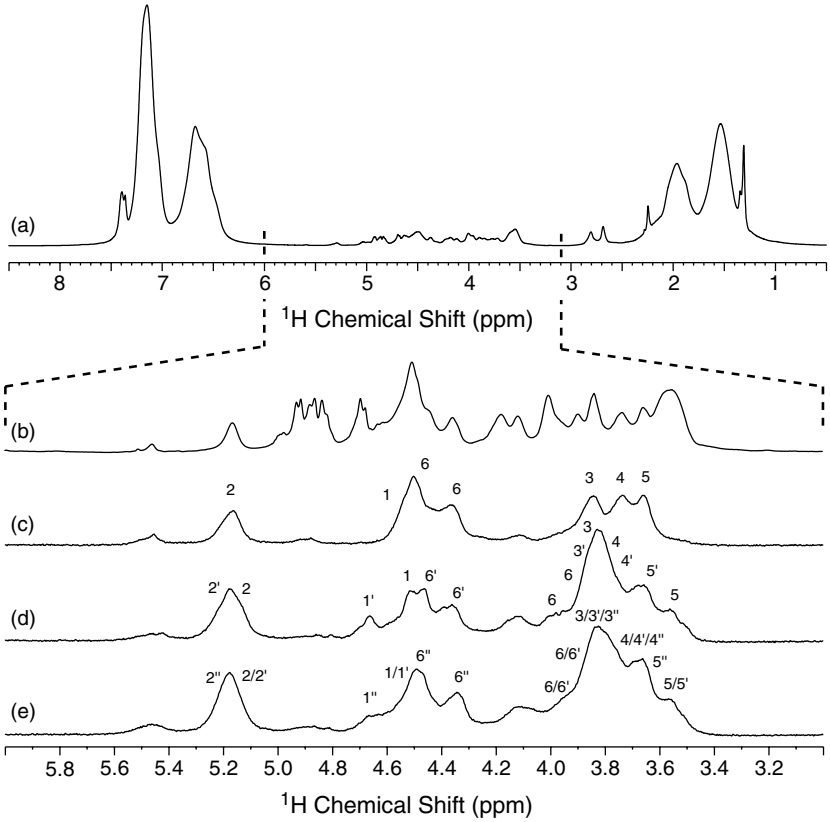

Figure 3. ^{1}H HR-MAS NMR spectra of the ^{13}C-labeled saccharide samples (**9**–**11**). As seen in spectrum (a), resonances arising from protons on the saccharide rings of **9** lie between 3 and 6 ppm; the large resonances outside of this region are due to the resin. An expanded view from a ^{13}C decoupled ^{1}H spectrum of **9** is shown in (b). To limit the observed signal to protons attached to labeled carbon sites, ^{13}C edited and decoupled ^{1}H spectra were acquired for **9**, **10** and **11** and are shown as spectra (c), (d) and (e), respectively. The seven peaks arising from protons directly bound to ^{13}C-labeled sites can be almost resolved in (c). The linewidths of the ^{1}H resonances are of the order of 50 Hz; this linewidth makes it impossible in spectra (d) and (e) to resolve all the resonances (14 are expected for **10** and 21 for **11**). The assignments were determined from ^{1}H–^{13}C HSQC spectra (see Fig. 6). Degenerate resonances are indicated by forward slashes.

2.5 ppm. The range of chemical shifts for the ^{13}C nuclei in the rings is not nearly so limited; peaks are dispersed over 45 ppm. Consequently, it is much easier to assign and interpret the ^{13}C spectra and then to use this information to assign the ^{1}H resonances. Figure 4(a) shows the ^{1}H decoupled ^{13}C spectrum for **9**. Resonances located below 60 and above 110 ppm are due to the natural abundance concentration of ^{13}C in the resin. The saccharide region of the ^{13}C spectrum is shown in Fig. 4(b), (c) and (d) for **9**, **10** and **11**, respectively. The six resonances that are expected for **9** can be clearly seen in Fig. 4(b) even though the resonances corresponding to carbons 2 and 5 are nearly degenerate. Some additional low-intensity peaks can be seen in this spectrum at 66–72 and 98 ppm. These resonances are due to saccharide molecules that are bound directly to the resin instead of to the octenediol linker. Although these impurities complicate the spectra to a certain extent, they do not affect the purity of the final synthesis product because they are not removed from the resin by the cleavage reaction.

To assign the ^{13}C resonances, we used the INADEQUATE experiment, which is well suited for working with linear spin systems. The arrows in Fig. 5(a) illustrate how it is possible to 'walk through' the INADEQUATE spectrum to assign the ^{13}C resonances for **9**. For **10** [Fig. 5(b)] and **11** [Fig. 5(c)], the INADEQUATE spectra can be analyzed in the same fashion. In the case of uniformly labeled samples, a number of additional peaks appear in the INADEQUATE spectra due to the generation of doubly antiphase coherences between three or even four spins. The four of these coherences that are most efficiently generated for **9** are indicated by dotted circles in Fig. 5(a); several weaker peaks that arise due to this mechanism appear at contour levels that are not visualized in the spectra shown in Fig. 5. Although both saccharide rings of **10** could be independently assigned, the close similarities between the first and second rings in **11** make most of the ^{13}C resonances from these two rings degenerate (at least within the limits of the experimental resolution). Resonance assignments that are degenerate are indicated by forward slashes in Figs 3, 4 and 6.

Once the ^{13}C resonances have been assigned, it is straightforward to use ^{1}H–^{13}C HSQC spectra to assign the ^{1}H resonances; such spectra are shown for the three samples in Fig. 6. The ^{13}C and ^{1}H resonance assignments that resulted from these experiments are given in Table 1.

^{13}C–^{13}C NOESY, ^{1}H–^{1}H NOESY and ^{1}H–^{1}H ROESY spectra of the samples did not reveal any cross peaks; we interpret this as an indication that the local environment of the saccharide molecules is dynamic, i.e. that the molecules

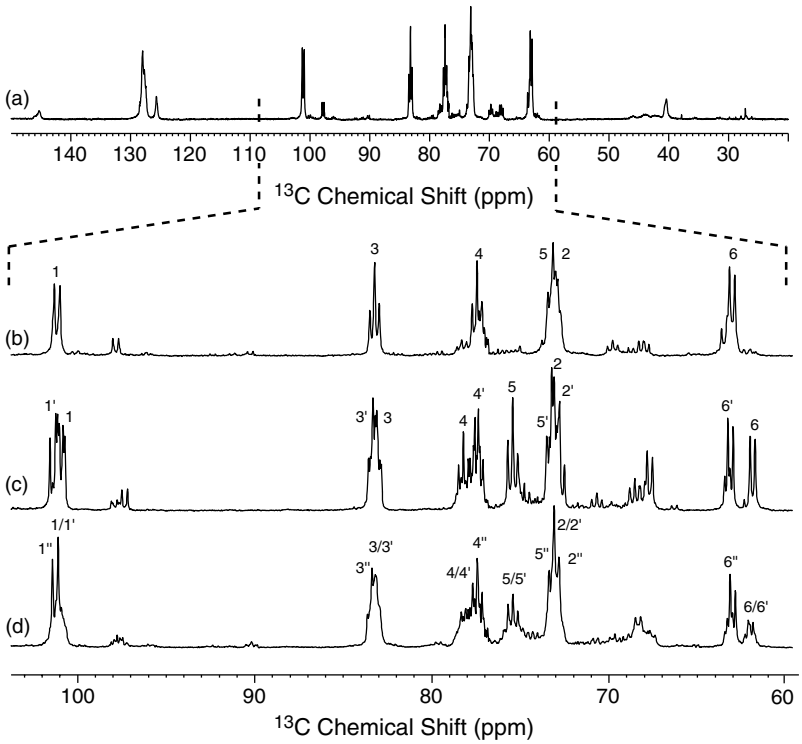

Figure 4. (a) ^{1}H decoupled ^{13}C HR-MAS NMR spectra of the ^{13}C labeled monosaccharide sample (**9**). The carbohydrate region of the spectrum for **9** is shown in (b); this same region is also shown for (c) **10** and (d) **11**. Spectral resonances above 120 and below 50 ppm are mainly due to the natural abundance concentration of ^{13}C nuclei in the resin. In spectra (b)–(d), the resonances at 98 ppm and between 66 and 72 ppm are due to impurities, as discussed in the text. The numbers give the assignments determined from the INADEQUATE spectra (see Fig. 5). Note that for **11**, several of the resonances are nearly degenerate and could not be disentangled in the INADEQUATE spectra; these degenerate resonances are indicated by forward slashes.

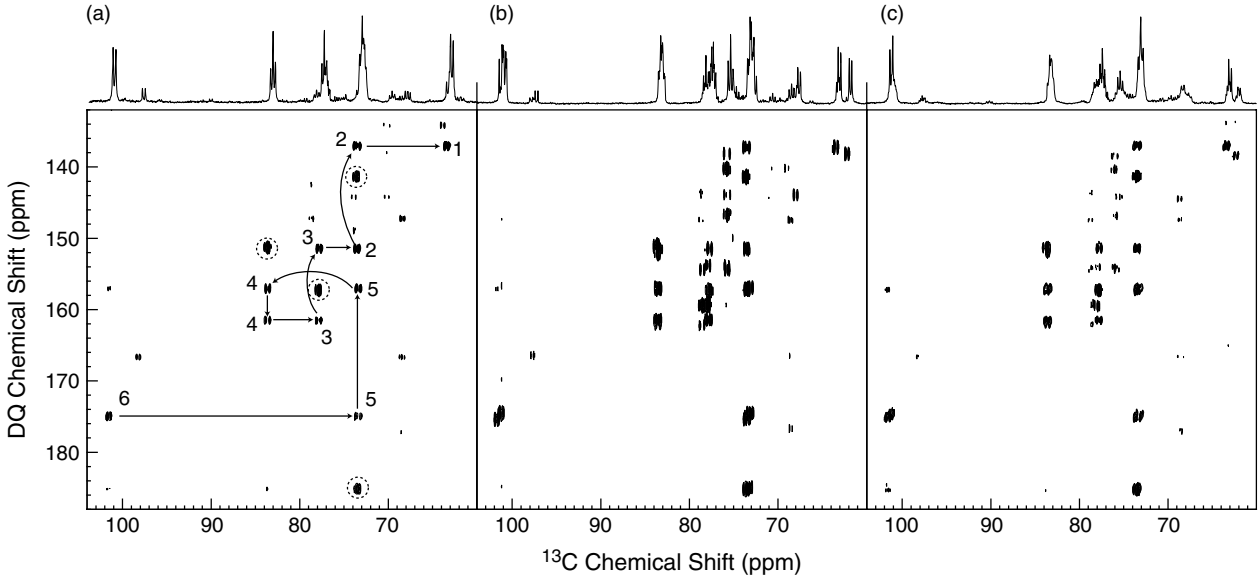

Figure 5. ^{13}C–^{13}C INADEQUATE spectra used for assigning the ^{13}C resonances for (a) **9**, (b) **10** and (c) **11**. In spectrum (a), arrows illustrate the coupling pathway connecting the resonances and dotted circles indicate strong cross peaks arising from three quantum spin order ($I_{1x}I_{2z}I_{3z}$). The other peaks seen in the spectra are due to ^{13}C-labeled impurities (as discussed in the text) and because of additional, less efficiently generated, three-quantum spin order terms.

do not have a well-defined structure when bound to the swelled resin. This interpretation correlates with the relatively short relaxation times that we observed for the saccharide resonances (T_1 = ~500 ms for ^{13}C and ~300 ms for ^{1}H).

It is often the case in HR-MAS NMR that better resolution of the desired resonances can be achieved by inserting a CPMG pulse train immediately before signal acquisition.[20,21] This takes advantage of the fast rate at which broad resonances dephase during the CPMG period.

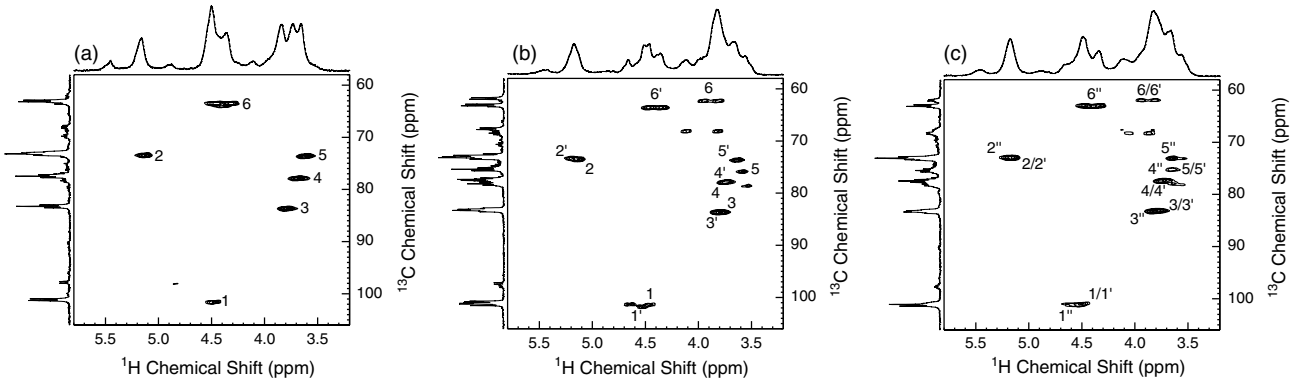

Figure 6. ^{1}H–^{13}C HSQC spectra for (a) **9**, (b) **10** and (c) **11**. The increase in spectral congestion with the addition of more saccharide rings is apparent going from spectrum (a) to (c). Degenerate peaks that cannot be resolved are indicated by forward slashes.

Narrow resonances are only slightly attenuated by the CPMG pulse train and, consequently, are enhanced relative to the broad signals in the resulting spectrum. The end result is that broad resonances are removed (or at least attenuated) in the spectrum and therefore the apparent resolution of the remaining resonances in the spectrum is improved. Unfortunately, the interesting resonances in our samples had relatively fast transverse relaxation times (i.e. they were the broad components of the signal), so this technique was not applicable.

CONCLUSION

By incorporating ^{13}C labels, we have succeeded in characterizing and assigning the ^{1}H and ^{13}C NMR spectra of resin-bound oligosaccharide samples. This highlights an important application of HR-MAS to the monitoring of solid-phase syntheses of ^{13}C labeled oligosaccharides, an application that is important in the synthesis of both uniformly and selectively labeled saccharides by solid-phase techniques. Such labeled materials are becoming increasingly important for studying the structure and function of oligosaccharides and glycoproteins in biological processes.

Table 1. Resonance assignments (in ppm) for the ring carbons and protons for the resin-bound saccharides **9**, **10** and **11**. The resins were swollen with $CDCl_3$, which was also used as the lock reference

	^{1}H (ppm)			^{13}C (ppm)		
Atom	**9**	**10**	**11**	**9**	**10**	**11**
1	4.47	4.52	4.51	101.2	100.9	100.8
2	5.11	5.16	5.15	73.0	73.2	73.2
3	3.77	3.81	3.80	83.2	83.2	83.3
4	3.66	3.78	3.77	77.4	77.6	77.7
5	3.59	3.65	3.64	73.2	75.4	75.8
6	4.43/4.30	3.97/3.85	3.95/3.83	63.1	61.9	62.0
1′		4.65	4.51		101.4	101.8
2′		5.20	5.15		72.8	73.2
3′		3.81	3.80		83.3	83.3
4′		3.76	3.77		77.4	77.7
5′		3.66	3.64		73.2	75.8
6′		4.48/4.36	3.95/3.83		63.2	62.0
1″			4.64			101.2
2″			5.19			72.9
3″			3.80			83.5
4″			3.75			77.5
5″			3.65			73.2
6″			4.49/4.34			62.9

Acknowledgments

The authors thank Dr Anthony Bielecki for assistance. N.M.L. thanks the National Institutes of Health for support via a National Research Service Award post-doctoral fellowship (F32 NS42425-01). P.H.S. gratefully acknowledges financial support from GlaxoSmithKline (Research Scholar Award), the Alfred P. Sloan Foundation (Scholar Award) and Merck. This work was supported in part by NIH NIBIB grant EB002026.

REFERENCES

1. Merrifield RB. *J. Am Chem. Soc.* 1964; **86**: 304.
2. Merrifield RB, Singer J, Chait B. *Anal. Biochem.* 1988; **174**: 399.
3. Caruthers MH. *Science* 1985; **230**: 281.
4. Seeberger PH, Haase W-C. *Chem. Rev.* 2000; **100**: 4349.
5. Seeberger PH (ed), *Solid Support Oligosaccharide Synthesis and Combinatorial Carbohydrate Libraries*. Wiley-VCH: New York, 2001.
6. Keifer PA, Baltusis L, Rice DM, Tymiac AA, Shoolery JN. *J. Magn. Reson. A* 1996; **119**: 65.
7. Sarkar SS, Gargipati RS, Adams JL, Keifer PA. *J. Am. Chem. Soc.* 1996; **118**: 2035.
8. Fitch WL, Detre G, Holmes CP, Shoolery JN, Keifer PA. *J. Org. Chem.* 1994; **59**: 7955.
9. Seeberger PH, Beebe X, Sukenick GD, Pochapsky S, Danishefsky SJ. *Angew. Chem., Int. Ed. Engl.* 1997; **36**: 491.
10. Kanemitsu T, Kanie O, Wong C-H. *Angew. Chem., Int. Ed. Engl.* 1998; **37**: 3415.
11. Kanemitsu T, Wong C-H, Kanie O. *J. Am. Chem. Soc.* 2002; **124**: 3591.
12. Mogemark M, Elofsson M, Kihlberg J. *Org. Lett.* 2001; **3**: 1463.
13. Mogemark M, Elofsson M, Kihlberg J. *ChemBioChem* 2002; **3**: 1266.
14. Mogemark M, Elofsson M, Kihlberg J. *J. Org. Chem.* 2003; **68**: 7281.
15. Shaka AJ, Keeler J, Frenkiel T, Freeman R. *J. Magn. Reson.* 1983; **52**: 335.
16. Shaka AJ, Keeler J, Freeman R. *J. Magn. Reson.* 1983; **53**: 313.
17. Bodenhausen G, Ruben DJ. *Chem. Phys. Lett.* 1980; **69**: 185.
18. Bax A, Freeman R, Kempsell SP. *J. Am. Chem. Soc.* 1980; **102**: 4849.
19. Morris GA, Freeman R. *J. Am. Chem. Soc.* 1979; **101**: 760.
20. Carr HY, Purcell EM. *Phys. Rev.* 1954; **94**: 630.
21. Meiboom S, Gill D. *Rev. Sci. Instrum.* 1958; **29**: 688.